JOURNAL OF MATERIALS SCIENCE **37** (2002) 41–49

Dispersion state and mechanical properties of core-shell particle modified epoxy networks

L. BECU, M. TAHA, A. MAAZOUZ*
Laboratoire des Matériaux Macromoléculaires UMR-CNRS 5627, Bât. 403, INSA, 69621 Villeurbanne Cedex, France

G. MERLE
Laboratoire des Matériaux Organiques à Propriétés Spécifiques UMR-CNRS 5041, Bât. IUT, Université de Savoie, 73376 Le Bourget du Lac Cedex, France

Dispersion of Core Shell particles (CS) in an epoxy network was analyzed by manual and automatic image processing methods yielding quantitative morphological indexes. These indexes were mainly based on the classical coefficient of variation, used for the statistics of the particles counted in a grid, or for the neighbor distances. The rubbery CS were either commercial or home made having different core nature, shell thickness and functionnalization (carboxy or epoxy). Two dispersion methods were used: a laboratory high speed mixer ("Ultraturrax"), or a co-rotating twin screw extruder with different screw profiles and temperature. The shell functionnalization was to be a key factor leading to high dispersion. Samples were taken along the extruder screws and analyzed. Multiple kneading blocs followed by reverse screw element were necessary for the obtention of a dispersion equivalent to the one obtained using the "Ultraturrax". The presence of particles (9.5 to 24% in volume) slightly decreased the quasi-static mechanical properties, that is Young's modulus and yield strength. On the contrary, toughness is enhanced, as expected, especially with functionnalized particles. In addition, the scatter on the fracture properties was directly related to the morphological heterogeneity index.

1. Introduction

There are two main procedures for generating a second phase dispersion in a thermosetting polymer. The first consists in addition of rubbers [1] or thermoplastics which are initially miscible in the epoxy systems and display a phase separation during curing [1–4]. Thus the final morphology of the dispersed phase is strongly dependent on curing conditions [5, 6]. Reactive liquid polymers with low molar masses based on carboxy-terminated butadiene acrylonitrile copolymers have been employed with great success but also result in appreciable loss in thermomechanical properties due to their partial miscibility with the epoxy resins [6, 7].

To avoid the loss of the thermomechanical properties of such materials, another way consists in using an initially miscible thermoplastic with a high T_g [8–11]. The main problem which arises from this addition is the control of the final morphology and consequently the thermodynamic parameters of the system (miscibility, curing, etc.). Moreover, the high level of toughness expected was not obtained [11].

To avoid these problems, a second way consists in dispersing an immiscible polymer in a pre-defined shape (powder or latex) into the epoxy matrix. These latexes are prepared by seed emulsion polymerization, which allows designing of well defined particles (ratio and chemical nature of core, shell and functional groups). Such pre-formed particles, which are of general use in toughened plastics [12], are the subject of increasing interest in the field of thermosets. Such three phase morphology gives excellent bulk properties, which can be explained through finite element simulation: according to [13], a particle having a rubber core and a plastic shell is believed to give good toughness improvement, by way of the main general toughening mechanism, i.e. matrix yielding.

Nevertheless few articles were devoted to the use of core-shell latexes (CS) as modifiers for thermoset resins, especially for epoxies [14–17]. In addition, structured core-shell particle agents provide model systems that allow independent examination of the role of the particle size, the particle to matrix interaction, and the cohesive strength of particles on the toughening mechanisms [18–20].

The mechanisms involved in the toughening depend on the intrinsic ductility of the matrix material [21], on the morphology of the blend, and on the properties of the CS particles such as particle size [22], chemical

---

*Author to whom all correspondence should be addressed.

0022–2461 © *2002 Kluwer Academic Publishers*

structure, and state of dispersion [23]. However the control of state of dispersion is essential in order to control subsequent mechanical properties. Nevertheless, most studies in the literature only address the increase of toughness and little progress has been made in controlling the state of dispersion in the final material [3]. Wu [24], in studying particle size effects in rubber toughened nylon, first suggested the existence of a critical interparticle distance (IPD) for optimum toughness. The interparticle distance for cooperative cavitation was considered an important toughening mechanism due to the overlap of the local elastic stress fields. On the other hand, it was suggested that the critical IPD should be a pure property of the matrix and independent of the particle size and volume fraction [25].

By Transmission Electron Microscopy (TEM), the examination of the deformation bands around a crack reveals the generation of a multiplicity of yield zones between particles [26]. Lu [27] performed a detailed study about the fracture of a series of epoxy networks of various crosslinking density, toughened by CS, using fractography: "particle cavitation is first initiated by the high stress concentration due to local stress fields overlap, i.e. particle interaction in the triaxial state. The formation of the croids starts from particle cavitation. The cavitated particles occur in line arrays, through which the crack propagate". For highly crosslinked systems, voids appear, caused by the failure of the particle-matrix interface, i.e. through particle debonding. "It is clear that debonding becomes easier when particles agglomerate", and "a crack can easily propagate through this highly damaged material without major energy consumption". In addition, another concluding remark of the author is the following: "When the interparticle distance is too small, it has an adverse effect on toughening".

For years, it has been observed that dispersion heterogeneity provides preferential tracks where cracks can pass through easily, and so the scatter in the measure of impact energy is a significant parameter [28]. For studying the hierarchy of the deformation in rubber toughened polycarbonate, Cheng [29] performed a multi-scale analysis: macro-, micro- and nano-scale. In this paper, the mutual interaction of particles is highlighted by the nano-scale examination of the zone ahead of the notch, where the cooperative cavitation produces linear array of cavitated particles. And so, the influence of the local environment of the particles (neighbor proximity, chains or strings) can be expected.

At larger scale, the clusters of particles can have opposite effects: promote the matrix plasticity or the fissure deviation, but, on the other hand, it has been noticed that composite toughness strongly increases with decreasing content of agglomerates larger than 10 μm [30]; in other words, the reinforcing effect of the particles is lost in the large clusters.

Hence, the quality of the dispersion drives the mutual interaction of particles, which is important in the deformation mechanisms. Nevertheless little research has been done on the measurement of the dispersion quality and its effect on mechanical properties of materials, apart from Brechet, who claims, in a general paper [31], that the histogram of the nearest neighbor distances should be a suitable parameter for describing the quality of dispersion homogeneity.

Literature is poor in methods and data concerning polymer blends and composites. Measurements of dispersion state can be found, by relative sizes of agglomerates to give a dispersion index [32] or by textured image processing [33]. A classical binary image processing result, the histogram of Voronoï distances, can be used [34]. A very similar method was used by Huang: the examination of the first neighbors by Thiessen tessellation: interparticle distances and angles, volume fraction, for subsequent stress analysis [35]. In this work, a dimensionless number, the first neighbor interaction index FNII (FNII $= (r_1 + r_2)/L$, between two particles of radii r_1, r_2, at distance L) appears to be an interesting parameter (but the particle size disappears as a parameter).

The particle size effect has to be taken into account for modeling the mechanical behavior [36], although the theoretical values of stress concentrations of a sphere are independent of its size, using normalized scales. We prefer to keep the particle size as a parameter. Besides, for a particle distribution which tends to be homogeneous, the distribution of the interparticle angles seems not to be crucial [35], so a complete tessellation method is not necessary, the classical way giving the nearest neighbor distances should be suitable.

In this context, this paper focus on the measurement of the dispersion, using characteristic values not only of averages (distances...) but also of their scatter. The state of dispersion, in relation with structure particles and processing conditions is discussed. The influence of state of dispersion on mechanical and toughness behaviors of the final materials is reported and discussed.

2. Experimental

2.1. Reagents

2.1.1. Epoxy network

The chemical reagents used are presented in Table I. A mixture of diglycidyl ether of bisphenol A (DGEBA) and dicyandiamide (Dicy) was used as the matrix. The catalyst used was benzyl dimethylamine. The aminohydrogen-to-epoxy ratio of 0.6 was chosen to obtain the maximum of the glass transition temperature, T_g (140°C for the fully cured neat epoxy matrix). The chemical pathways and the resulting architecture of such a network were described in another paper [7].

2.1.2. Core-shell particles

Different core-shell latexes (Table I) were considered. The core-shell particles denoted CS1 and CS2 are from Rohm and Haas. The CS1 were based on a poly(butadiene co styrene) core and a poly(methyl methacrylate) shell functionnalized with carboxy groups (CS1a) or not (CS1b). The particles denoted CS2 were based on a poly(butyl acrylate) core and a poly(methyl methacrylate) shell functionnalized with carboxy groups (CS2a) or not (CS2b). In both cases, the shells were slightly crosslinked. For studying better

TABLE I Chemicals used in synthesis of materials

Name	Chemical formula	Supplier
DGEBA	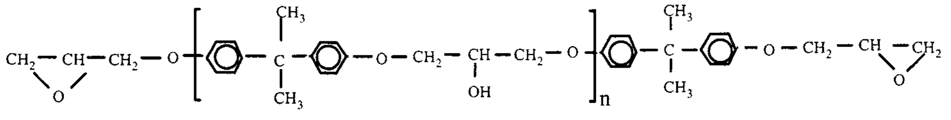 $\overline{Mn} = 380\ gmol^{-1}$	Bakelite 0164
Dicy	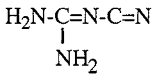 $H_2N\text{-}\underset{\substack{\vert\\ NH_2}}{C}\text{=N-C=N}$ Dicyandiamide	Bakelite VE 2560
BDMA	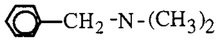 Catalyst or initiator	Aldrich
CS particles	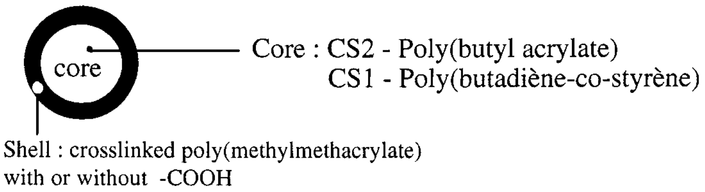	Rohm & Haass EXL 2600 2611

the effect of the particles structure on the dispersion state, other model particles, home made and denoted CS3, were studied. They were based on a poly(butyl acrylate) core and a shell of poly(methyl methacrylate) functionnalized (CS3a) or not (CS3b) with glycidyl methacrylate (GMA). The chemical pathways and the resulting structure of such particles were described in another paper [14].

TABLE II

Experiment N°	Screw profile	Extrusion temperature (°C)	CS nature
1	A	60	CS1a
2	A	90	CS1a
3	B	60	CS2b
4	B	90	CS2b
5	B	60	CS2a
6	B	90	CS2a
7	B	60	CS1b
8	B	90	CS1b
9	B	60	CS1a
10	B	90	CS1a

2.2. Processing of CS/epoxy blends

Two means were used to mix DGEBA prepolymer, hardener Dicy, and the core-shell particles:

a. A high speed mechanical stirring using a "Ultra-turrax" T50 mixer operating at 2800 rpm.

b. A Clextral BC 21 intermeshing co-rotating twin-screw extruder ($D = 25$ mm, $l = 900$ mm). CS/Dicy/BDMA were first dry-blended and fed into the extruder hopper. The epoxy prepolymer (DGEBA) was pumped into barrel 2. The extruder drive was run at the desired speed. It took approximately ten minutes for output, pressure and temperature to be stabilized. Then the extrudate was taken. In the case where samples were to be removed for morphological studies, the extruder screw rotation was stopped and the cooling system of all barrels switched on. At the same time the barrels, positioned on a bar driven by a hydraulic jack, were quickly removed and specimens taken from the superior side of screws. For Residence Time Distribution (RTD) studies, diphenyl was used as a UV tracer, 0.5 g was injected, as an impulse in the field hopper to the extruder. Samples were collected from the extruder die, dissolved in THF, filtered and analyzed by SEC with a UV detector at 254 nm. The RTD characteristics were calculated using the tracer concentration at time t (C_t) as described previously [37, 38]. The extrusion conditions were reported in Table II. In all extrusion and Turrax mixing experiments, 24 vol% CS were used. The Amine/Epoxy molar ratio was 0.6, the catalyst concentration was 1 wt% in respect to epoxy. The screw profiles used in this study were reported in Fig. 1. The cure schedule of the blend was one hour at 120°C, followed by one hour at 180°C. The detailed procedure was similar to that used in a previous study [7]. During curing, the mold rotated, in order to prevent possible sedimentation of the CS particles and Dicy.

2.3. Experimental techniques for characterization

2.3.1. *Microscopy*

The morphology of the particles and their ability to be dispersed in the reactive epoxy mixture were checked by transmission electron microscopy (TEM) using a Hitachi HV12 microscope. Osmium tetraoxide vapor was used to stain the epoxy continuous phase on 10–80 nm thick samples for 24 hours, whereas, an aqueous solution of phosphotungstic acid (1 wt%) was used to stain the core (polybutadiene or poly(butyl acrylate) of the CS particles.

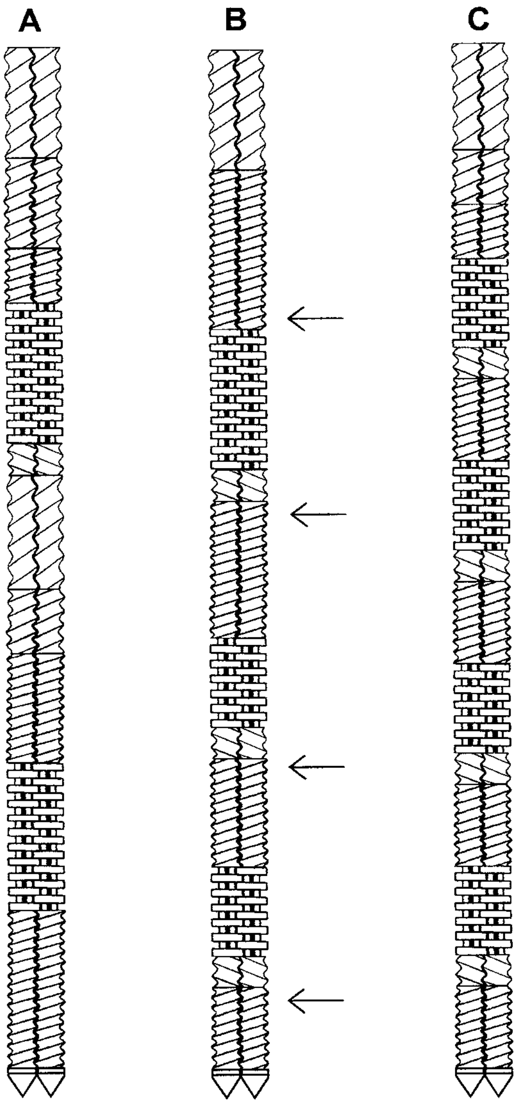

Figure 1 Screw profiles A and B (arrows indicate sampling location).

2.3.2. Image analysis

2.3.2.1. Eyes and hand inspection method. The TEM pictures have some imperfections: the particle can debond under the cutting blade, consequently the corresponding hole appears in white near the particle which is darker than the resin matrix (Fig. 2, see also later Fig. 5, Fig. 6). This aspect is well understood visually, the whole particle being well recognized. This is another kind of problem for automated image analysis. Thus it is efficient to process manually (either directly counting, or touch up the image for subsequent automated processing). The TEM photographic pictures are blown up to be more easily handled. A spreadsheet holding a grid of 32 boxes is put on the image, then we count in every box the particle number and the interparticle connection number. The size of the box is about 20 times the particle diameter. The sample size is about 300–500 counted particles. The counts yield: average particle number by box, average connection number by box, and the corresponding standard deviations. (If the dispersion is perfectly homogeneous, the standard deviation is equal to zero.)

- The variation coefficient of the particles number population is very sensitive to the dispersion

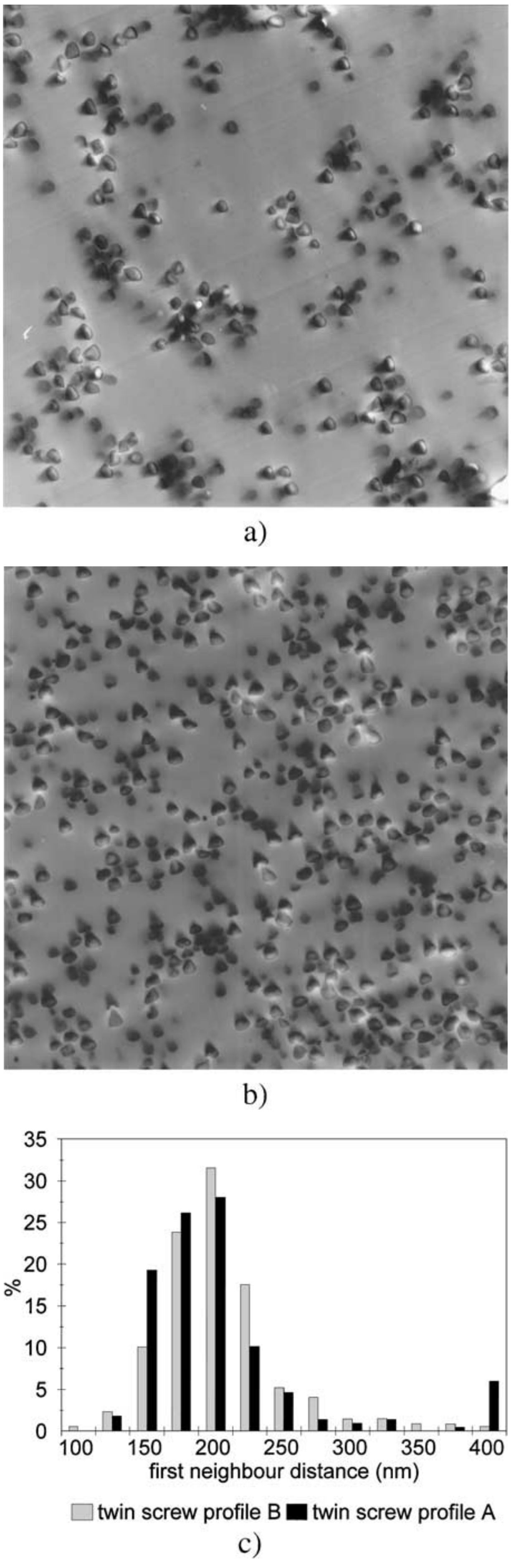

Figure 2 Examples of dispersion having the same average first neighbor distance; (a) dispersion obtained with the screw profile A, (b) dispersion obtained with the screw profile B (side length of the images: 6 μm), (c) corresponding histograms.

quality. Its value is a hundred times the ratio of the standard deviation to the average. We chose such a classical statistics parameter as the dispersion heterogeneity parameter for the particles number: DHn, dimensionless.

– The same for the links: DHl.

– The average links number by particle is also a parameter representative of the strings and clusters tendency.

This is a semi-global approach, at the micro-scale (which depends on the size of the analyzing grid).

2.3.2.2. Digital. The image analysis system was composed of a 512 × 512 square pixel CCD camera (PULNIX TM 760), a frame grabber (Digital Vision Cyclope) and home-made software. In order to perform local analysis (at the nano-scale, in the immediate vicinity of each particle) automatic processing is chosen.

The gray scale images are transformed into binary ones by thresholding, eventually after again a "eye and hand recognition," faster and more suitable than an automatic segmentation in the case where particles appear differently from each other due to the slicing effects. The sample size is about 600–800 counted particles.

Classical image processing gives the First Neighbor Distance for each particle. The distribution of the values gives a global view of the dispersion, as is shown hereafter for two examples (Fig. 2). Nevertheless our goal is not to replace an image (microscopy) by another image (histogram). In summary, we chose simple characteristic values for dispersion quality: the distribution parameters used are:

1. The distances average (we call it FND).

2. The distribution scatter, characteristic and very sensitive to the dispersion quality. For that we use again the variation coefficient, and we chose it as the dispersion heterogeneity parameter (DH, dimensionless), it reveals the width of the distribution.

In addition in this case the histogram reveals that the broadest distribution shows higher values of distances; for that, the higher order distribution parameters could be used.

A complementary value is defined, that is the first neighbor proximity (FNP), which is the average of the reciprocal values of the first neighbor distances (the unit is a spatial frequency). This parameter is similar to the FNII. We prefer it to the IPD, because the closer neighbor is to the particle, the more pronounced is the interaction, and the higher is the FNP.

The product FND · FNP is equal to 1 for perfectly regular dispersion, its practical value is higher. We choose it as a dispersion index (DI, dimensionless).

DI against DH (Fig. 3) illustrates the behavior of the dispersion, that is the smaller are the values, the better is the dispersion. The presence of isolated particles increases more DH than DI. On the other hand, the tendency to agglomeration of the particles (strings) increases more DI than DH. Such a graph can summarize the comparison of a lot of images (including different effects on dispersion quality, see later). Notice that such an analysis is performed at micro-scale, in comparison to the previous one. In particular, a perfect string will give DH = 0 and DI = 1. If contradictory effects seem to appear between DH and DI, it means that the analysis is too local, and then the other parameters such as DHn have to be taken into consideration. When the dispersion is quite regular, as in the case of CS1a, a good correlation ($R = 0.99$) is found between DHn and DH.

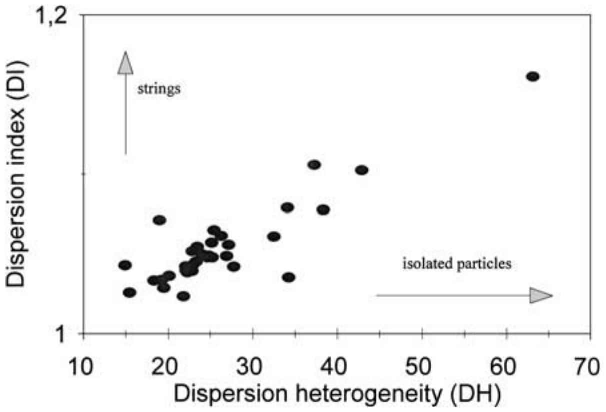

Figure 3 Dispersion index versus dispersion heterogeneity: synthetic diagram for all the dispersions studied.

2.4. Mechanical testing

Tensile and fracture tests were performed using a Adamel Lhomargy DY25 at room temperature. The measurements were performed on ISO 60 specimens. The strain was recorded using strain gauges at a crosshead speed of 10 mm · min^{-1}. Thus, Young's *moduli*, E_{RT}, and Poisson ratios, υ, were determined for all materials.

The plastic strain behavior of the neat matrix and the CS-modified epoxies was also studied using the same tensile machine equipped with a compression device. Yield stresses, σ_{y} , and yield strains, ε_{y}, were then measured.

Fracture toughness (critical strain energy release rate, G_{IC}, and the critical intensity factor, K_{IC}), were measured according to the procedure developed by the European Group on Fracture of Polymers [39]. All measurements were performed on single-edge notched three-point bending specimens (60 mm × 14 mm × 7 mm). The span was 56 mm. A crosshead speed of 10 mm · min^{-1} was used. At least, five samples were fractured to obtain the average value of K_{IC}, from the maximum load at failure. As is known, not only the average but also the dispersion of the results are independent values from any determination. So, we gave the variation coefficient (see the results thereafter, Table IV).

3. Results and discussion

The dispersion quality of CS particles in epoxy reactive systems depends mainly on the interparticle interactions, particle matrix interactions and also the mixing conditions. Concerning the pictures of particle dispersion, both ours and those presented in the literature, the general comments are:

- a perfect dispersion is never encountered;
- the non appropriate dispersion conditions produce clusters and aggregates;
- at low scale (in the range 10–100 times the particle diameter), the ratio particles/matrix varies significantly;
- very often, the particles tend to remain stuck together, which leads to strings.

3.1. Effect of the interparticle interactions

In a first part, dispersion experiments of different home made CS particles in epoxy were made. In order to maintain mixing constant conditions, a laboratory "Ultraturrax" was used. Since CS were synthesized by emulsion polymerization, a surfactant was used [14]. At the reaction end, water was taken off by lyophilisation and the obtained CS still contained the surfactant, sodium dodecyl sulfate (SDS). SDS can be extracted by water washing. To analyze the effect of SDS on CS dispersion state, experiments were made using non-washed and washed CS. As shown in Fig. 4, a correct dispersion was obtained for purified CS while agglomerated particles were obtained with non purified CS. This agglomeration phenomenon is probably due to hydrophobic SDS sequences interactions. In order to avoid such phenomenon, only purified CS were used for the rest of this study. The main parameters concerning the CS structure that can have potential influence on dispersion in reactive systems are the shell thickness and its nature. One of the shell roles is to give shape and integrity to the CS particle. Minimizing the shell thickness, an incomplete shell can be obtained. As shown in Table III, such decrease of shell ratio going from 30% to 10% results in lower dispersion quality. In addition, Lu *et al.* showed that plasma treatment of particle surface resulted in higher dispersion (we have processed these images to quantify this effect). This can be explained by a functionnalization of the CS shell. In this study unfunctionnalized and functionnalized shells (carboxy and epoxy) were dispersed in epoxy reactive systems. Results given in Table III show considerable dispersion improvement using functionnalized shells. This effect can be explained by higher physical interactions of functionnalized CS with epoxy resins. The twin screw extruder produces a similar result, illustrated by TEM pictures, Fig. 5 (the study of the mixing conditions is on the following).

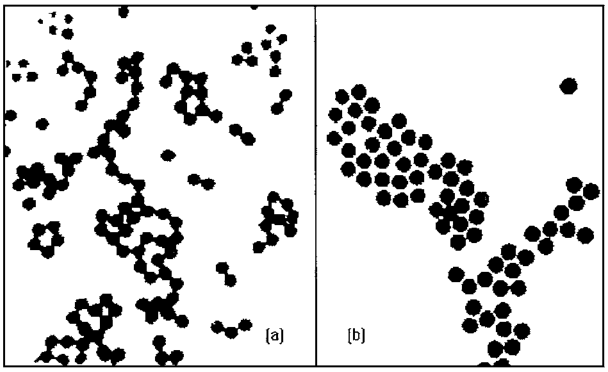

Figure 4 Surfactant effect on dispersability: (a) before and (b) after washing.

TABLE III Effect of core characteristics on dispersion quality

Effect of relative core thickness

Type of particle	Ratio shell/core (%)	DHn	DH	DI	Link/ particle
CS3	30	25	20	1.036	0.5
CS3	17	32	19	1.034	0.78
CS3	10	42	21	1.12	0.81

Effect of shell treatment

Type of particle	Surface treatment	DHn	DH	DI	Link/ particle
Lu [27]	/	42			
Lu [27]	Plasma	25			
CS3b	/	30	25	1.048	0.41
CS3a	Epoxy	22	22	1.039	0.21
CS1b	/	60	15	1.050	0.9
CS1a	Acid	9	18	1.033	0.01

3.2. Mixing parameters influence

It was shown that an "Ultraturrax" can be successfully used for CS dispersion. Such a mixing tool cannot reasonably be used for industrial purpose. For this reason experiments were made in order to examine the possibility of continuous dispersion of CS in epoxy resin using a co-rotating closely intermeshing twin screw extruder as an industrial tool. In a first part, screw profile A was designed and used. This profile contained two kneading disc blocks, the first one was followed by a left handed screw element. The presence of this element increasing the residence time of materials within the kneading blocks, increasing their dispersion possibility.

3.2.1. Screw profile optimization

Screw profile C was first used in order to examine the morphology evolution along the screws. This profile was designed with four kneading disc areas, the 2nd, 3rd and 4th were followed by a small left handed screw element. Experiments were made at 90°C using CS functionnalized or not (CS2a and CS2b respectively). Samples were taken on points 1, 2 and from the extruder die, cured and analyzed by SEM and image analysis.

The dispersion of the non functionnalized CS is not correct and an increase of mixing going from point 1 to the die did not result in a better dispersion. On the contrary, higher agglomeration was observed. The rather good dispersion obtained with functionnalized CS was improved with shearing in point 2 and at the extruder die, as shown in Fig. 6.

The experiments show clearly the influence of functionnalization on the CS dispersion confirming the preliminary results of the preceding paragraph and that highly dispersive profile should be used to obtain a correct dispersion. Nevertheless, using the "simpler" B profile, an equivalent dispersion was obtained at the die ($DH = 14$). For that reason, profile B was used for the rest of this study.

3.2.2. Extrusion temperature

The blend viscosity is also a mixing parameter, that is a higher matrix viscosity can improve the particles

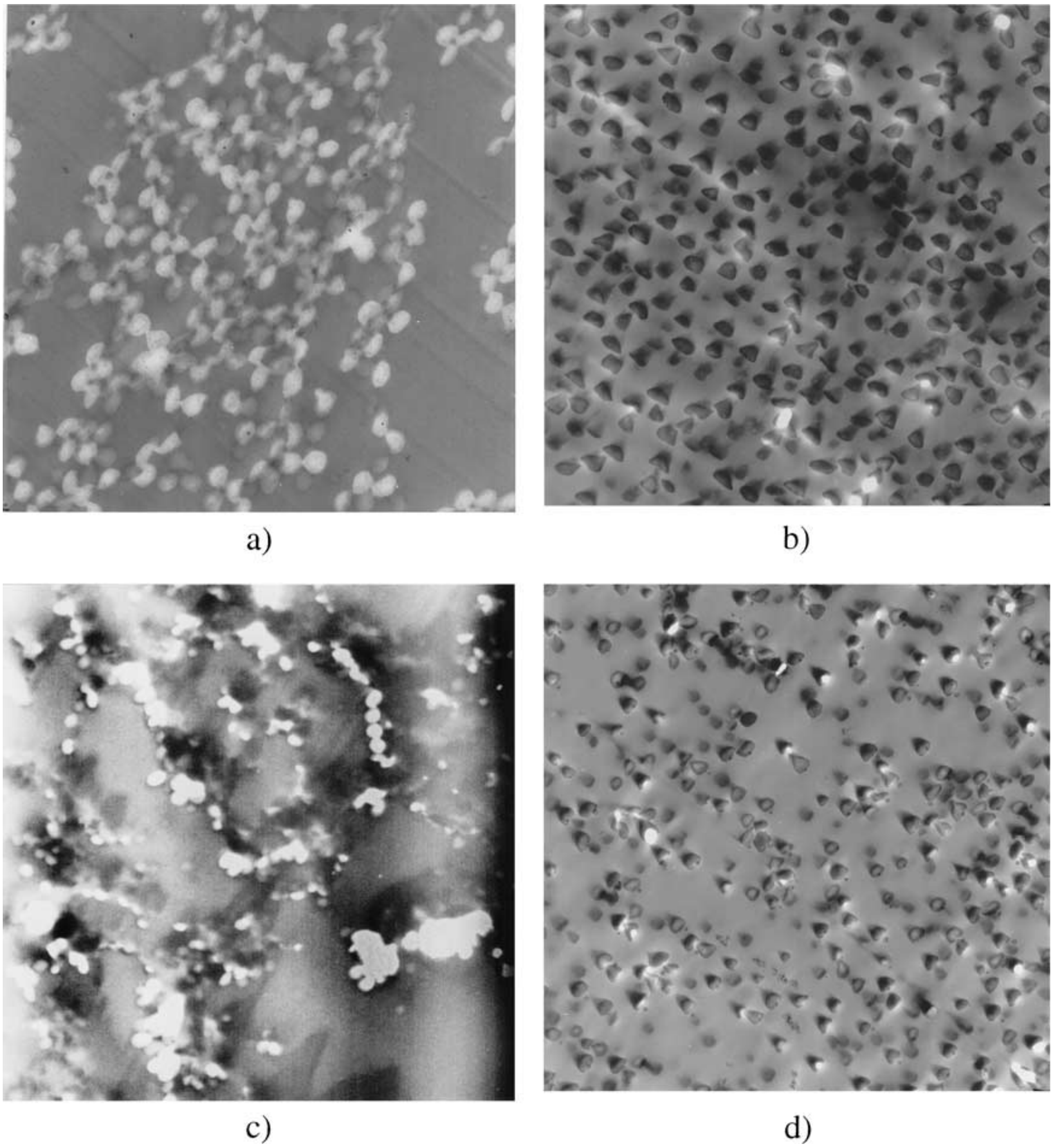

a) b) c) d)

Figure 5 TEM pictures of dispersions obtained using CS2 particles functionnalized (*b*, *d*) or not (*a*, *c*), and comparison between Ultraturrax (*a*, *b*) and extruder (*c*, *d*) (side lengths, *a*, *b*: 4.4 μm; *c*: 10 μm; *d*: 5.6 μm).

dispersion. Using screw profile B, experiments were conducted at two barrel temperatures at 60 and 90°C and screw rotation rate of 250 rpm (exp. N° 9 and 10).

Specimens were taken from the extruder die. Amine was then added as hardener and the resin cured. TEM images corresponding to these experiments are given in Figs 5d and 2b (respectively 60 and 90°C). Even if in both cases a good dispersion was obtained, the experiment made at 60°C led to a better dispersion than that conducted at 90°C. The visual impression was confirmed by image analysis (see Fig. 7 thereafter).

3.2.3. Comparison between the mixing processes

The different indexes morphology are summarized on the Fig. 7, for the three extruder cases. The comparison with the "Turrax" shows the possibility to obtain good dispersion quality, using adapted extrusion conditions.

3.3. Mechanical properties

Becu *et al.* [14] recently showed that DSC analysis reveals glass transition temperature of 141 ± 2°C for all materials, indicating no change in chemical structure of the epoxy matrix via CS particles introduction. As expected, the Young's modulus at room temperature E, slightly decreases on introducing core-shell particles (Table IV). Actually, according to different mechanical models, the addition of a component having a low modulus to a glassy polymer tends to decrease its stiffness. However the values are more sensitive to the volume fraction than to dispersion state. The yield stress,

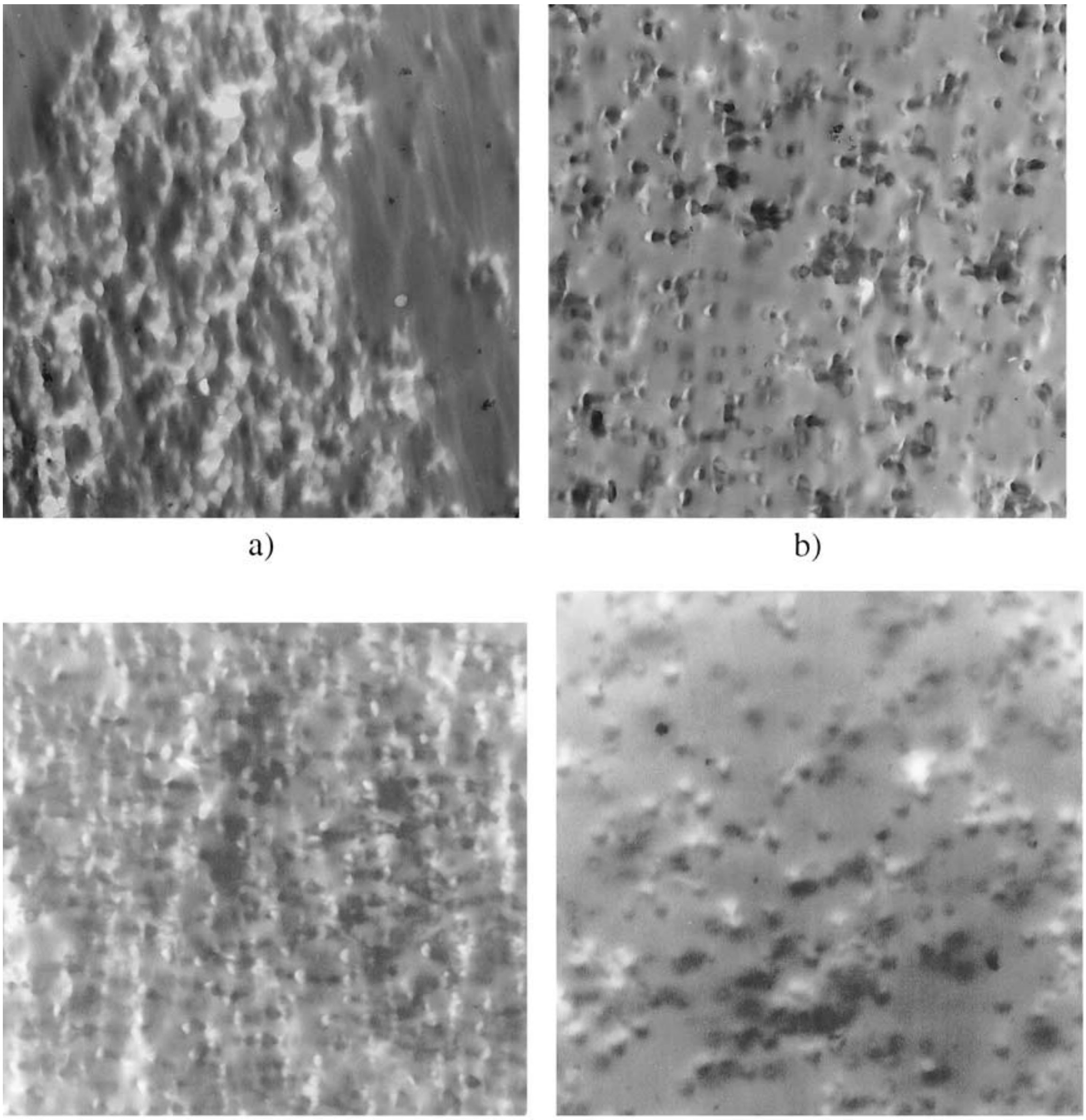
a)
b)
c)
d)

Figure 6 TEM pictures of samples taken along the twin screws; (a) sample taken at the point 1, (b) point 2, (c) point 3, (d) point 4 (side length: 5 μm).

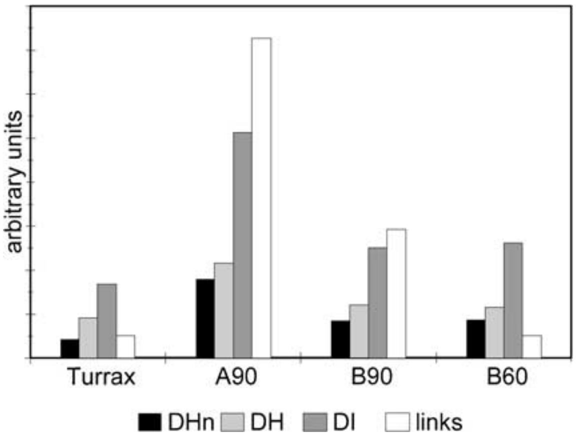

Figure 7 Comparison of mixing methods by using measurements from image analysis (lower values indicate better dispersion).

σ_y, is also sensitive to the presence of soft particles in epoxy matrix (Table IV). The analysis of yielding for similar systems in different testing modes (tension, compression, shearing, and a plain strain compression) shows that the same mechanisms are involved in the deformation process of the CS-modified epoxies [40]. Thus, the presence of the core shell particles favors the plastic deformations of the surrounding epoxy network, especially for the same good dispersion state. However, it's clear in our study that the dispersion state of CS particles had an influence on fracture properties (K_{IC}, G_{IC}).

As shown in Table IV, the materials exhibiting a high level of agglomeration (CS1b, CS2b, CS3) with large DHn show greatly dispersed K_{IC} values. More precisely, the correlation coefficient between the K_{IC} variation coefficient and the corresponding DHn value equals 0.89 for the set of the trials. Only functionnalized (CS1a, CS2a, CS3a) particles (DHn $\sim$ 10) confer a large improvement with a small standard deviation of the K_{IC} values. For 24% volume fraction, K_{IC} increases from 1.3 ± 0.5 MPa $\cdot$ m$^{1/2}$ for CS1b (DHn = 60) to 1.4 ± 0.1 MPa $\cdot$ m$^{1/2}$ for CS1a (DHn = 10). The same evolution was observed for the other materials.

TABLE IV Mechanical properties of CS particles modified epoxy networks

Composition of material	Modifier content (vol%)	E (GPa)	σ_y (MPa)	G_{IC} (J/m^2)	K_{IC} (MPa $\cdot$ m$^{1/2}$)	Variation coeff. on K_{IC}	DHn
Pure epoxy	0	3.0	101 ± 1	220	0.79	10	
Epoxy + CS1a	9.5	2.7	95 ± 3	490	1.11	5	28
Epoxy + CS1a	17.5	2.6	85 ± 2	450	1.10	7	30
Epoxy + CS1a	24	2.2	72 ± 1	800	1.4	7	9
Epoxy + CS1b	24	2.1	53 ± 2	1100	1.3	38	60
Epoxy + CS2a	24	2.2	71	1130	1.7	5	10
Epoxy + CS2b	24	1.8	84 ± 2	1030	1.3	38	50
Epoxy + CS3a	24	2.5	74 ± 10	400	1.5	3	22
Epoxy + CS3b	24	2.5	84 ± 2	830	1.1	7	25

4. Conclusion

An image processing technique for characterizing the dispersion state of core shell particles in epoxy matrix and its quantification has been applied successfully by using transmission electron microscopy images. Four indexes have been set to characterize the dispersion state, at the scale of the influence zone of each particle. Two of them are based on the distribution of the first neighbor distances, and at higher scale, two other based on an "eye and hand" recognition method. Mixing and compounding process, as well as the modification of the shell surface, play an important role in controlling the morphology of dispersed phase. More precisely, after studying the main parameters for a twin screw extruder (that is screw profile and temperature), the same good level of dispersion as when using a laboratory high speed mixer can be obtained. The quality of the particle dispersion has a great influence on the fracture properties of the CS particle modified epoxy networks. In particular, the dispersion of the toughness values appears to be correlated with a poor particle dispersion at mesoscale.

References

1. J. SULTAN and F. McGARRY, *Polym. Eng. Sci.* **13** (1973) 19.
2. W. BASCOM, R. TING, R. J. MOULTON, C. K. RIEW and A. R. SIEBERT, *J. Mater. Sci.* **16** (1981) 1657.
3. A. F. YEE and R. A. PEARSON, *ibid.* **21** (1986) 2475.
4. A. C. CARG and Y. W. MAI, *Comp. Sci. Technol.* **31** (1988) 179.
5. S. MONTARNAL, J. P. PASCAULT and H. SAUTEREAU, in "Rubber Toughened Plastics," Adv. Chem. Ser. 222, Vol. 8, edited by C. K. Riew (ACS, New Orleans, 1989).
6. D. VERCHÈRE, J. P. PASCAULT, H. SAUTEREAU, S. M. MOSHIAR, C. C. RICCARDI and R. J. J. WILLIAMS, *J. Appl. Polym. Sci.* **42** (1991) 701.
7. A. MAAZOUZ, H. SAUTEREAU and J. F. GÉRARD, *Polym. Networks Blends* **2** (1992) 65.
8. C. B. BUCKNALL and I. K. PARTRIDGE, *Polymer* **24** (1983) 639.
9. R. A. PEARSON and A. F. YEE, *ibid.* **34** (1993) 3658.
10. R. A. PEARSON, in "Rubber Toughened Plastics," Adv. Chem. Ser. 233, edited by C. K. Riew and A. J. Kinloch (ACS, Washington D.C., 1993) p. 405.
11. E. GIRARD-REYDET, V. VICARD, J. P. PASCAULT and H. SAUTEREAU, *J. Appl. Polym. Sci.* **65** (1997) 2433.
12. "Acryloid Impact Modifiers," Product brochure MR 119, Rohm and Haas Co. (1984).
13. T. KOJIMA, Y. KIKUCHI and T. INOUE, *Polym. Engng. Sci.* **32**(24) (1992) 1863.
14. L. BECU, H. SAUTEREAU, A. MAAZOUZ, J. F. GÉRARD, M. PABON and C. PICHOT, *Polym. Adv. Technol.* **6** (1995) 316.
15. G. LEVITA, A. MARCHETTI and A. LAZZERI, *Makromol. Chem., Makromol. Symp.* **41** (1991) 179.
16. Y. C. CHEN, V. DIMONIE and M. S. EL-AASSER, *Macromolecules* **24** (1991) 3779.
17. H. J. SUE, J. L. BERTRAM, E. I. GARCIA-MARTIN, J. W. WILCHESTER and L. L. WALKER, *Colloïd Polym. Sci.* **272** (1994) 456.
18. M. S. EL-AASSER, I. SEGALL and V. L. DIMONIE, *Macromol. Symp.* **101** (1996) 517.
19. D. S. KIM, K. CHO, J. K. KIM and C. E. PARK, *Polym. Eng. Sci.* **36**(6) (1996) 755.
20. J. Y. QIAN, R. A. PEARSON, V. L. DIMONIE and M. S. EL-AASSER, *J. Appl. Polym. Sci.* **58** (1995) 439.
21. A. J. KINLOCH, M. L. YUEN and S. D. JENKINS, *J. Mater. Sci.* **29** (1994) 3781.
22. D. DOMPAS and G. GREENINCKX, *Polymer* **35** (1994) 4743.
23. Y. SUETESUGU, in MOFFIS Symposium, Mineral and Organic Functional Fillers in Polymers, Namur, Belgium, 1993, preprint, p. 37.
24. S. WU, *Polymer* **26** (1985) 1855.
25. *Idem.*, *J. Appl. Polym. Sci.* **35** (1988) 549.
26. P. A. LOVELL, A. J. RYAN, M. N. SHERRAT and R. J. YOUNG, in Polymat 94, The Institute of Materials, London, September 1994, preprint, p. 578.
27. A. F. LU, Ph.D. thesis, Ecole Polytechnique Fédérale de Lausanne, Switzerland, 172p., 1995.
28. L. SUSPÈNE, J. F. GÉRARD and J. P. PASCAULT, *Polym. Eng. Sci.* **30**(24) (1990) 1585.
29. C. CHENG, A. HILTNER, E. BAER, P. R. SOSKEY and S. G. MYLONAKIS, *J. Appl. Polym. Sci.* **55** (1995) 1691.
30. V. SVEHLOVÁ, in Proceedings of the 28th Microsymposium on Macromolecules, "Polymer Composites," Prague, Czechoslovakia, July 1985, edited by B. Sedlàček (Walter de Gruyter, Berlin, 1986) p. 607.
31. Y. J. M. BRECHET, *Mater. Sci. Eng.* **A175** (1994) 63.
32. PH. COCHET, P. BARRUEL, L. BARRIQUAND, J. GROBERT, Y. BOMAL and E. PRAT, Meeting of the Rubber Division, ACS, Orlando, USA, 26–29 October 1993.
33. L. GANESAN, P. BHATTACHARYYA and A. K. BHOWMICK, *J. Appl. Polym. Sci.* **56** (1995) 1739.
34. H. YANG and J. S. COLTON, *Polym. Compos.* **15**(1) (1994) 46.
35. J. HUANG, Y. SHI and A. F. YEE, "Polymeric Materials" (ACS, Anaheim, 1995) p. 258.
36. F. DOLAN, D. TAYLOR and P. A. BLACKIE, in Polymat 94, The Institute of Materials, London, September 1994, preprint, p. 593.
37. C. TITIER, J. P. PASCAULT, and M. TAHA, *J. Appl. Polym. Sci.* **59** (1996) 415.
38. P. CASSAGNAU and M. TAHA, *ibid.* **60** (1996) 1765.
39. J. G. WILLIAMS, in "Fracture Mechanics of Polymers," edited by Ellis Horwood (Chichester, UK, 1987).
40. A. MAAZOUZ, H. SAUTEREAU and J. F. GÉRARD, *Polym. Bull.* (*Berlin*) **33** (1994) 67.

Received 21 March
and accepted 10 August 2001